AIAA 81-1863R

Entry Vehicle Performance in Low-Heat-Load Trajectories

Keith A. Havey Jr.*
Rockwell International, Downey, California

This paper shows the impact of low-stagnation-heat-load trajectories on the crossrange capabilities of gliding entry vehicles. Minimum heat load is achieved by following a peak deceleration profile for most of the trajectory, as defined by heating, dynamic pressure, and G load constraints. The ballistic parameter was 10-1000 lb/ft^2 and the lift-to-drag (L/D) ratio 1.5-2.5 for this completely parametric study. Results show that this type of trajectory does not necessarily reduce crossrange capability when compared with equilibrium glide solutions. The ballistic parameter and L/D required to satisfy a crossrange and heating constraint can be readily selected.

Nomenclature

D	= drag/mass
f	= steering function ($\dot{Q}, G$, or q)
G	= load factor
H_s	= scale height, ft
h	= enthalpy, Btu/lb
i	= orbital inclination, deg
K_l	= linear gain constant
K_r	= rate gain constant
$L/D, C_L/C_D$	= lift-to-drag ratio
Q	= stagnation heat load, Btu/ft^2
$\dot{Q}$	= stagnation heat rate, Btu/ft^2·s
q	= dynamic pressure, lb/ft^2
R_N	= vehicle nose radius, ft
S	= surface arc range, ft
T	= temperature, R
V	= atmospheric relative velocity, ft/s
W/C_DA	= ballistic parameter, lb/ft^2
W/C_LA	= lift loading, lb/ft^2
X	= downrange, ft
Y	= crossrange, n.mi.
ϵ	= emissivity
γ	= flight path angle, rad
ρ	= atmospheric density, slugs/ft^3
σ	= bank angle, deg

Subscripts and Superscripts

a	= actual value
c	= circular orbit
d	= desired value
f	= final
G	= constant load factor
i	= initial
l	= local condition
min	= minimum
nom	= nominal
o	= total
$\dot{Q}$	= constant heating rate
q	= constant dynamic pressure
s	= stagnation point condition
w	= wall
∞	= freestream
$'$	= first derivative with respect to time

Presented as Paper 81-1863 at the AIAA Atmospheric Flight Mechanics Conference, Albuquerque, N. Mex., Aug. 19-21, 1981; submitted Sept. 30, 1981; revision received April 9, 1982.

*Member Technical Staff, Advanced Systems (presently with Eastman Kodak Company, Rochester, N.Y.). Member AIAA.

Introduction

In order to minimize the thermal protection system (TPS) weight requirement for any entry vehicle, it is necessary to incorporate aeroheating analysis with the trajectory shaping process. It has been shown that the minimum system weight results when the entry trajectory shape is based on the temperature characteristics of the TPS under consideration, in contrast with generating a trajectory and then selecting a TPS for the vehicle.[1,2] The former method results in a reduced total heat load, or time at temperature, to which the vehicle is exposed. For an insulative TPS this should also reduce the total TPS weight requirement. Generating this type of trajectory is a relatively straightforward procedure. However, a crossrange requirement may also be imposed on the vehicle, and this results in a more difficult trajectory shaping problem.

In response to this, two objectives of this study were selected:

1) To show the effect of the ballistic parameter (W/C_DA) and lift-to-drag (L/D) ratio on crossrange for low-heat-load trajectories.

2) To assist in the selection of the W/C_DA and L/D needed to satisfy vehicle constraints on peak heating rates or temperatures, dynamic pressure, and load factor while satisfying a mission crossrange requirement, all for low-heat-load trajectories.

The type of information given here is new in the sense that such detailed analyses of low-heat-load trajectories have not been shown before. Numerous authors have given details for equilibrium glide trajectories and others have presented useful information for minor circle turn maneuvers.[2-5] Additional detailed entry trajectory analysis methods are available.[6-16] Most of these publications provide good parametric data for specific types of trajectories; however, the desire to minimize TPS weight may result in a need for several different flight segments for an entry trajectory, as illustrated in the following paragraphs.

A typical entry flight regime envelope is illustrated in Fig. 1. Any entry vehicle will have constraints that define the corridor through which it can fly. The flight ceiling is defined by an equilibrium glide trajectory with the vehicle in a maximum lift, 0 deg bank angle attitude. For a controlled, nonskip entry trajectory the flight ceiling represents the highest altitude the vehicle can attain at any velocity. The flight floor is defined by heating and air loads or G constraints on the vehicle and represents the lowest altitude the vehicle can safely attain at any velocity.

The lowest heat load will generally occur if the vehicle flies along the flight floor, since there the drag and deceleration are maximized, resulting in the shortest entry flight time. This type of trajectory is illustrated by the dashed line in Fig. 1. After a deorbit burn the vehicle maneuvers for pullout along a

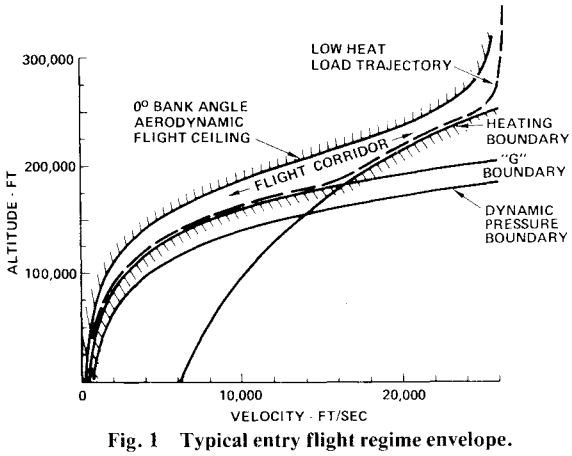

Fig. 1 Typical entry flight regime envelope.

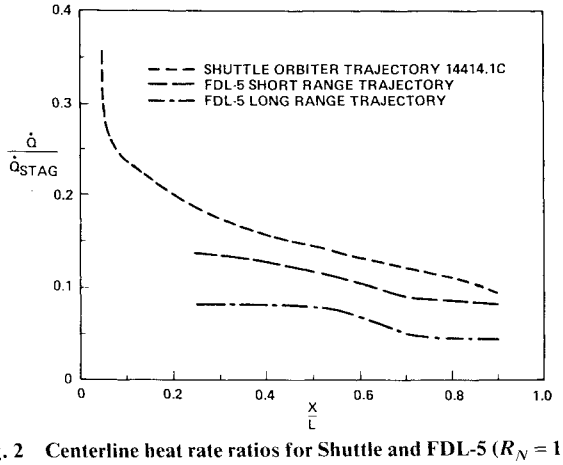

Fig. 2 Centerline heat rate ratios for Shuttle and FDL-5 (R_N = 1 ft).

constant heating rate profile. At this point the angle of attack and/or bank angle are used to modulate the vertical component of lift so that the vehicle stays on the heating boundary. This constraint is followed until a G or dynamic pressure q limit is reached. (With angle-of-attack modulation both limits may be reached at some point in the trajectory.) The guidance then switches to keep the vehicle within this new constraint. Finally, after completing a 90 deg heading change, the vehicle departs from this boundary and maneuvers to a 0 deg bank angle, maximum L/D configuration to maximize the crossrange.

The trajectories generated for this analysis were restricted in four ways. First, the angle of attack was held constant throughout the trajectory, and therefore only the bank angle was used to control the vehicle. This assumption allows the generation of an entry trajectory early in the design stage of a vehicle, since it eliminates the need to define any vehicle-specific aerodynamics. This also results in a simplification of any aeroheating calculations since the vehicle flowfield and local heating rates are strong functions of angle of attack. The second and third restrictions were on the aerodynamic load factor and the dynamic pressure. The load factor was limited to 3 G and the dynamic pressure was held to 300 lb/ft^2. These limits were selected since they are in line with current vehicle loading and acceleration constraints for entry flight. The impact of these assumptions will be discussed later. For the fourth restriction, the heating time has been ignored. It is assumed that the heating limit selected for constant heating rate flight could be sustained indefinitely. Or in other words, any TPS overtemperature capabilities or limitations are being ignored. This has no major impact on the analysis as presented here, but it does significantly influence trajectory flexibility and TPS material selection.

This type of trajectory also has potential limitations that could develop such as the early onset of turbulent heating and high combined structural and thermal loads, as will be discussed later. But it does provide low stagnation heat load while satisfying three important vehicle constraints.

It is important to note that the expression "low heat load" as used in this paper does not necessarily mean that very high heat rates are encountered during entry. It simply means that the vehicle flys along some predetermined maximum heat rate for most of the trajectory, followed by transition to a G or q limit and a glide profile. This yields approximately the lowest heat load based on the heating limit selected. In contrast, the "minimum-heat-load" trajectory would result if the vehicle flew on the heating rate profile corresponding to the maximum temperature capability of the TPS, followed by flight along the maximum G or dynamic pressure limit all the way to landing.

Heating and Temperature Prediction

The stagnation heating rate equation used for this analysis is given in Eq. (1).[17] Note that this equation includes a factor $(1-h_w/h_0)$ which takes into account the reduction in heating rate due to a nonzero wall temperature.

$$\dot{Q}=17{,}700\left(\frac{\rho}{R_N}\right)^{1/2}\left(\frac{V}{10^4}\right)^{3.07}\left(1-\frac{h_w}{h_0}\right) \tag{1}$$

where

$$h_w=0.24\,T_w$$

$$h_0=(0.24\,T_\infty+V^2/50{,}063)$$

The wall temperature T_w is a function of the heating rate and can be found from the Stefan-Boltzmann Law as,[18]

$$\dot{Q}=\epsilon K_{SB}\,(T_w^4-T_\infty^4)$$

where

$$K_{SB}=0.476\times10^{-12}\text{Btu/s}\cdot\text{ft}^2\cdot R^4$$
$$=\text{Stefan-Boltzmann constant}$$

Since the wall temperature during early entry flight is typically several times the local atmospheric temperature, this term can be ignored. After some rearranging of the constant K_{SB} Eq. (2) from which the wall temperature can be found results,

$$\dot{Q}=0.476\times\epsilon\,[T_w/1000]^4 \tag{2}$$

In addition to knowing the heating rate at the stagnation point, it is helpful to find a relationship for the actual surface temperatures that could be expected during entry. In Fig. 2 typical laminar centerline heating rates for the Shuttle orbiter and for the FDL-5 reusable spacecraft configuration are illustrated.[19,20] The Shuttle heating data shown are from the TPS design trajectory 14414.1C. (This is an 1100 n.mi. crossrange abort entry from a 104 deg inclination orbit, with a 40/30 deg angle-of-attack schedule.) For these two vehicles, $\dot{Q}_l/\dot{Q}_s\leq0.2$ for $x/L\geq0.2$. With this information and from similar relationships, it can be shown that for laminar flow and angles of attack less than or equal to 30 deg the local heating rate at $x/L=0.2$ along the body centerline will be approximately 20% or less of that at the stagnation point.[21] An examination of Shuttle orbiter and FDL-5 constant temperature contours shows that approximately 75% of the vehicle lower surface will be at $Q_l/Q_s\leq0.2$. Next, Eq. (2) can be used to relate local heating rates to surface temperatures.

Assuming a temperature limit of 2000°F and an emissivity of 0.8, a local heating rate of 13.95 Btu/ft$^2\cdot$s results. Since

the local-to-stagnation heat rate ratio equals 0.2, this in turn gives a stagnation point heating rate of 13.95/0.2 or 69.73 Btu/ft^2·s (for a nose radius of 1 ft) on which to guide the entry vehicle. By limiting the vehicle to this heating rate, the resulting local temperatures on 75% of the body will be less than or equal to 2000°F.

It must be understood that this is only an approximate relationship to be used for preliminary trajectory shaping. Once a vehicle has been designed the actual flowfields, heating rates, and temperatures must be determined and a new trajectory generated if the temperature predictions were significantly in error. For turbulent heating constraints it may be necessary to generate segments of the trajectory at a lower laminar local-to-stagnation-point heating rate ratio, and thus the vehicle will encounter a more benign entry environment.

Configuration/Vehicle Characteristics

If the equations of motion for gliding flight are examined, it is apparent that these can be rearranged such that the weight W, drag coefficient C_D, lift coefficient C_L, and reference area A always occur in the combinations of W/C_DA and C_L/C_D (or L/D). For a parametric study of the type presented here this is particularly useful since it eliminates the need to define any vehicle characteristics other than the ballistic parameter and lift-to-drag ratio. For this study W/C_DA was 10-1000 lb/ft^2 and L/D 1.5-2.5.

W/C_DA and L/D were selected in a systematic way for each trajectory flown so that a known stagnation point heating rate would not be violated. Equation (3) was developed to show the approximate effect of lift loading, W/C_LA or $(W/C_DA)/(L/D)$, orbit inclination, and bank angle on the peak stagnation point heating rate encountered during entry from low Earth orbit.

The equation as shown here was derived from the equations of motion in combination with Eq. (1) for the stagnation heating rate and assumed that $(1-h_w/h_0)=0.95$. Except for the term showing the effect of orbit inclination on the heating rate, this result is very similar to that reported by B.A. Galman.[15]

$$\dot{Q}=\left[\left(\frac{39.88-11.78\cos i}{R_N}\right)\left(\frac{W}{C_LA}\right)\left(\frac{1.125}{0.125+\cos\sigma}\right)\right]^{1/2} \quad (3)$$

assuming

$$\gamma \text{ at } 400{,}000 \text{ ft} \leq 3 \text{ deg}$$

$$V \text{ at } 400{,}000 \text{ ft} \simeq 26{,}000 \text{ ft/s}$$

$$-95 \leq \sigma \leq 95 \text{ deg}$$

Figure 3 illustrates the results of this equation for several inclinations and bank angles. Equation (3) provided the basis for selecting W/C_DA and L/D. After a heating rate, inclination, and bank angle are selected, the lift loading can be found as shown in Fig. 3. Since the lift loading relates to ballistic parameter and lift-to-drag ratio as shown earlier, W/C_DA and L/D can now be selected to satisfy the heating constraints. For the analysis here the inclination was assumed fixed at 90 deg and the bank angle in the equation was varied from 0 to 75 deg by increments of 15 deg. However, the general effect of entry from inclinations other than 90 deg on crossrange is discussed later.

Guidance Method

As mentioned earlier, the lift-to-drag ratio and thus the angle of attack was assumed to be constant for the entire trajectory. This assumption becomes less accurate for Mach numbers near 5 and below; but it is a conservative estimate with respect to crossrange, since the crossrange generated after this point is generally less than 1% of the total.

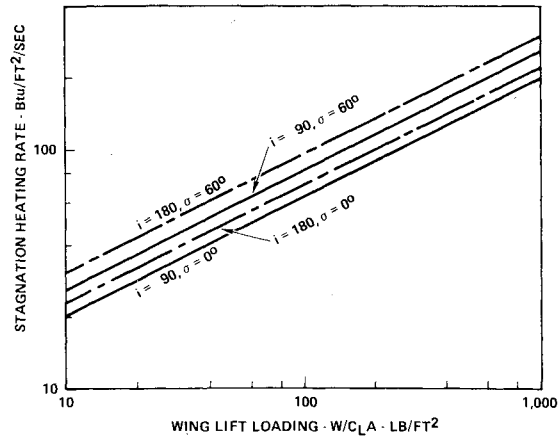

Fig. 3 Minimum stagnation heating rates for lifting entry vehicles ($R_N=1$ ft, $\epsilon=0.8$).

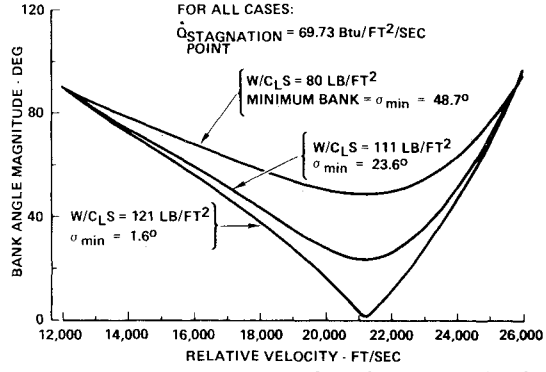

Fig. 4 Approximate bank angle schedules for constant heating rate entry trajectories.

The bank angle flown was found from a linear feedback steering model as given in Eq. (4). The linear gain constants used were approximately -1, -10, and -100 for constant dynamic pressure, heating rate, and load factor flight, respectively. The rate gains for each type of flight were an order of magnitude larger, -10, -100, and -1000, given in the same order. These values were selected based primarily on experience with the Program to Optimize Simulated Trajectories (POST).[22]

$$\sigma=\sigma_{\text{nom}}+K_f(f_a-f_d)+K_r(f_a') \quad (4)$$

The nominal bank angle is found from a closed-form solution as a function of velocity, vehicle characteristics (L/D and W/C_DA), and the desired value of the steering function, f (i.e., heat rate, dynamic pressure, or G load). All of these functions relate to the quantity ρ^aV^b (where a and b are constants), and thus the required vertical component of lift, $L\cos\sigma$ (a function of ρV^2), can be defined.[23] The linear feedback model makes corrections to the bank angle based on the magnitude and rate of change of errors in the steering function.

Constant heating rate flight is followed first during entry (see Fig. 1). Typical bank angle schedules for this flight mode are shown in Fig. 4. For a given heating rate, increasing the lift loading reduces the magnitude of the bank angle at any given velocity (below V_c). The minimum bank angle that will occur can be predicted quite accurately by selecting the lift loading, inclination, and the desired heating rate and solving Eq. (3). The minimum bank angle will occur at a velocity dependent on the orbit inclination, typically about 20,000 ft/s for a 0 deg inclination and 23,000 ft/s for a 180 deg inclination. (This assumes that the atmosphere rotates with the Earth at a velocity of about 1500 ft/s.)

Constant dynamic pressure and constant load factor G flight are achieved in a similar manner to constant heating rate flight (i.e., the lift required to hold the steering function constant is defined by a closed-form solution). To transit between flight modes the dynamic pressure and load factor were monitored by the entry program until their actual value was within about 5% of their maximum. At this point the new steering function (dynamic pressure or G) and new gain constants were defined to follow this flight profile.

Gliding flight was used after the vehicle had changed its heading by 90 deg. A bank rollout rate of 5-10 deg/s was performed until a 0 deg bank was achieved. The vehicle then glided at a 0 deg bank until the flight was terminated at a velocity of 2500 ft/s.

Trajectory Generation

All flights started at a velocity of 26,000 ft/s and an inclination of 90 deg. However, the altitude, flight path angle, latitude, and longitude had to be selected. The flight path angle for constant heat rate flight can be defined from a closed-form solution as

$$\gamma_{\dot{Q}} = -6.14 H_S (D/V^2) \tag{5}$$

The altitude was determined by solving Eq. (1) for density at the desired heating rate and by assuming an exponential atmosphere with a scale height of 23,500 ft. The initial latitude and longitude were selected so that landing would always be in the central United States. In order to define these initial coordinates, the total range that could be flown had to be estimated.

Crossrange was predicted based on the equilibrium glide solution, and downrange was estimated by calculating the surface arc range and subtracting the crossrange component. The following equations were used to predict the total range flown.

Constant heat rate:

$$\Delta S_{\dot{Q}} = \left[\frac{(W/C_D A)}{\dot{Q}^2}\right]\left[\frac{V_i^{6.14} - V_f^{6.14}}{888^{6.14}}\right] \tag{6}$$

The constants for this equation came from Eq. (1) assuming that $(1 - h_w/h_0 = 0.95)$.

Constant load factor:

$$\Delta S_G = \left[1 + \left(\frac{L}{D}\right)^{2}\right]^{1/2}\left[\frac{V_i^2 - V_f^2}{32.174 * G}\right] \tag{7}$$

Constant dynamic pressure:

$$\Delta S_q = \left[\frac{(W/C_D A)}{q}\right]\left[\frac{V_i^2 - V_f^2}{32.174}\right] \tag{8}$$

Equilibrium glide crossrange:

$$\Delta Y = 217 \times (L/D) + 533 \times (L/D)^2 - 48.2 \times (L/D)^3 \tag{9}$$

Total range:

$$\Delta X = [(\Delta S_{\dot{Q}} + \Delta S_{G,q})^2 - (\Delta Y \times 6076.1)^2]^{1/2} \tag{10}$$

The constants for the equilibrium glide equation came from a curve fit of the results given by Bell and Slye extrapolated for a 90 deg inclined orbit.[3,4] The constant 6076.1 in Eq. (10) converts nautical miles to feet to keep the units consistent.

The Program to Optimize Simulated Trajectories (POST) was used to generate all trajectories.[22] POST is a point mass, three-degree-of-freedom program ideally suited for this type of problem. The equations needed to calculate the bank angle for the entry guidance are contained within a subroutine of this program. A rotating Earth model and the 1962 standard atmosphere options from the POST program were used.

Results

Figure 5 illustrates the crossrange capabilities as a function of ballistic parameter, lift-to-drag ratio, and heating rate. Each family of curves represents a particular heating or temperature limit. Within these families, the near-vertical lines follow identical minimum bank angles and bank angle schedules (see Fig. 4) and the dome-shaped curves (horizontal direction) lines of constant L/D. The most obvious feature is that for any temperature limit and L/D there is a single ballistic parameter which maximizes the crossrange for this type of trajectory.

An examination of these curves shows that the crossrange attained is primarily a function of L/D and the minimum bank angle for the lower two heating rates, whereas at a heating rate of 127.4 Btu/ft^2·s there is an increase in crossrange capability. This shift could be shown to occur when the ballistic parameter is greater than $100\sqrt{1 + (L/D)^2}$ since above this number the dynamic pressure limit of 300 lb/ft^2 is attained before the 3 G limit. This can be reasoned from an examination of Eq. (11) defining the load factor for gliding flight with no side factor for gliding flight with no side force,

$$G = \frac{q}{W/C_D A}\sqrt{1 + (L/D)^2} \tag{11}$$

were reached, a dynamic pressure greater than 300 lb/ft^2 would result. This q increase would reduce the total range flown, as can be shown by Eq. (8). Therefore, the increased crossrange shown in Fig. 5 for higher $W/C_D A$ is consistent with this information. However, note that accompanying the increased range is an increase in flight time and total stagnation heat load as well.

By cross-plotting the data presented in Fig. 5, constant crossrange profiles can be generated (see Fig. 6). This shows the same type of result, only in a somewhat more usable manner. If a crossrange is specified, then the combinations of L/D and $W/C_D A$ needed to satisfy this requirement can be read directly from the graph. Since the heat load is proportional to $W/C_D A$ (see Fig. 7), the lowest practical value of $W/C_D A$ would be most desirable to minimize the insulative TPS weight requirement.

Downrange increases with increasing ballistic parameter and with increasing lift-to-drag ratio. However, since the deorbit point for an entry vehicle can be selected as necessary to satisfy a particular downrange, this is not a primary

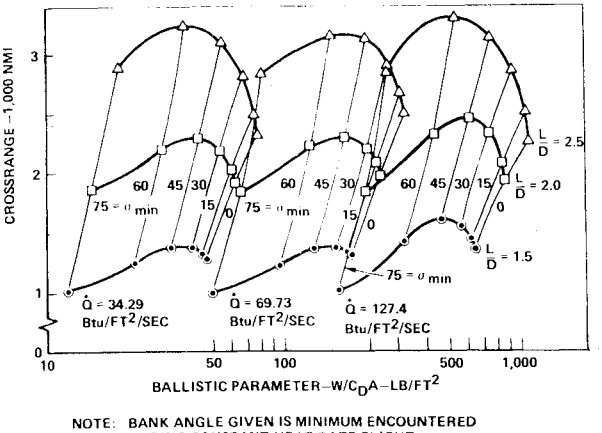

NOTE: BANK ANGLE GIVEN IS MINIMUM ENCOUNTERED DURING CONSTANT HEAT-RATE FLIGHT

Fig. 5 Crossrange capabilities in low-heat-load trajectories.

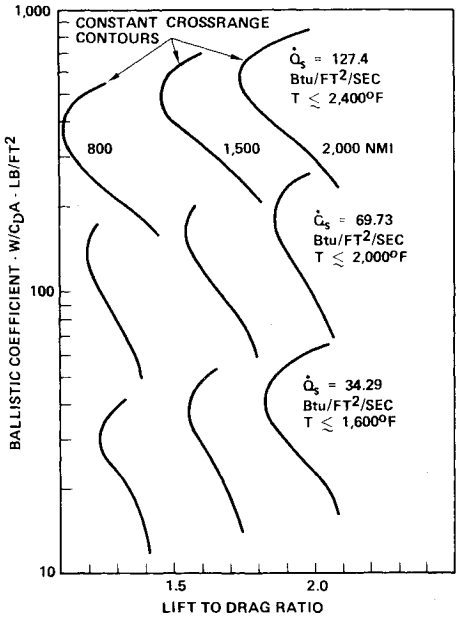

Fig. 6 Selection of W/C_DA and L/D to satisfy crossrange and temperature limits.

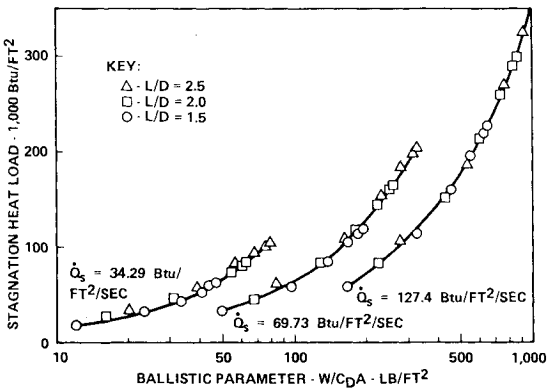

Fig. 7 Effect of ballistic parameter and stagnation heat rate on total heat load ($R_N = 1$ ft, $\epsilon = 0.8$).

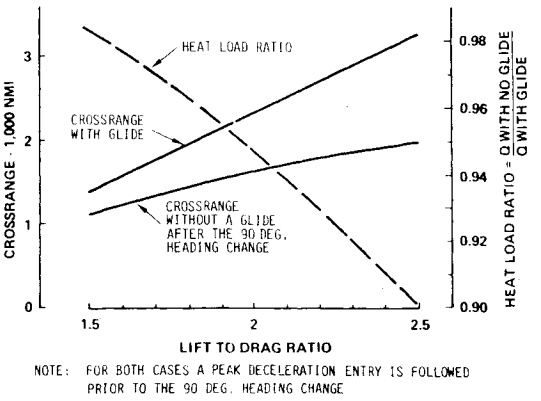

Fig. 8 Comparison of 0 deg bank angle glide flight with a 3 G flight segment after achieving a 90 deg heading change.

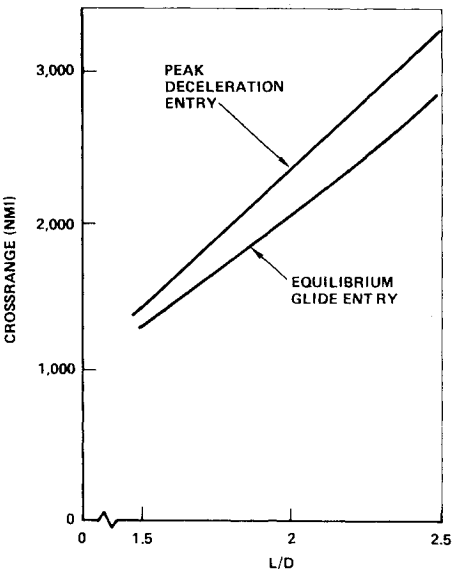

Fig. 9 Comparison of peak deceleration and equilibrium glide crossrange capabilities (3 G max).

consideration when designing a vehicle for a crossrange requirement.

Analysis

Since several values for lift-to-drag ratio and ballistic parameter will satisfy vehicle constraints and mission requirements (Fig. 6), a trade must be made between these two parameters while considering actual vehicle design limitations. For example, to satisfy a payload volume requirement a large vehicle cross section may be needed, and consequently a higher drag configuration (lower L/D) would result. Also, an increasing L/D as occurs on the lower half of each crossrange curve is an indication of a larger vehicle surface area, and thus the area requiring TPS increases. Consequently, the total vehicle weight may increase. Because of these volume, weight, and L/D interactions, the minimum L/D point for a given crossrange and temperature requirement becomes a likely "first cut" design point for an entry vehicle.

As an alternative to the 0 deg bank angle flight segment at the end of this trajectory, a constant G profile was also examined to determine the impact of this final trajectory segment on vehicle performance. The changes in maximum crossrange capability and heat load are as shown in Fig. 8. For $L/D = 2.5$, the reduction in crossrange amounts to about 39%. The heat load reduction is about 10%. The exact reductions should be found from an analysis related to a mission requirement, such as the crossrange. For example, if the crossrange is set at 2000 n.mi (for the 2000°F case in Fig. 6), the L/D required for entry with a final glide trajectory segment is about 1.86. W/C_DA is 185 lb/ft² and the resulting heat load is about 135,000 Btu/ft². If the peak deceleration profile is used with the same crossrange requirement, the L/D required is about 2.52 and the heat load is about 121,000 Btu/ft². Thus, the heat load decreased about 10% but a 35% increase in L/D was required. This large change in L/D indicates that the glide maneuver is preferred for this phase of the entry flight.

Figure 9 shows a comparison of the maximum crossrange cases for these trajectories with the crossrange generated in equilibrium glide trajectories with identical lift-to-drag ratios. The crossrange for maximum deceleration profiles compares favorably with glide-type trajectories. However, when the total stagnation heat loads are compared (see Fig. 10), the deceleration trajectory becomes much more favorable.

Curve fits of some of these data were made to assist in the extrapolation of this information to vehicles with various combinations of L/D and W/C_DA. These fits were made after a close examination of Fig. 5 indicated that a good correlation of the data could be expected. The results are valid for $1.5 \leq L/D \leq 2.5$, and for vehicles limited to 3 G. Although

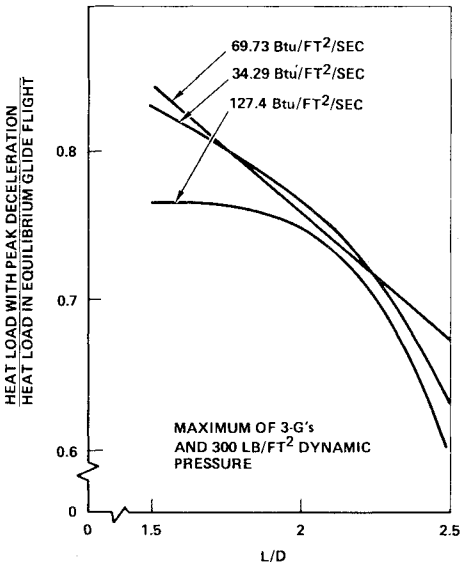

Fig. 10 Heat load reduction from flying a peak deceleration entry.

no curve fitting of data for the 300 lb/ft^2 dynamic pressure limited curves was made, the general trends shown here in Figs. 5-7 can be used to estimate the impact of this constraint on vehicle performance. Extrapolation of these data outside of the given ranges can be made within "reasonable" limits and should not provide any major inaccuracies; however, more data are needed to verify these trends positively.

The desired minimum bank angle for the best crossrange performance (as shown in Fig. 5) for a peak deceleration entry is essentially independent of ballistic parameter for a given L/D, and can be estimated with

$$\sigma_d = 19.25 * L/D + 7.52 \tag{12}$$

The lift-to-drag ratio needed to satisfy a crossrange requirement for this type of trajectory is

$$(L/D)_d = (C + 1357)/1820 \tag{13}$$

The ballistic parameter can be specified once a heating rate limit is established by rearrainging Eq. (3) to form

$$\left(\frac{W}{C_D A}\right)_d = \frac{\dot{Q}_d^2 R_N^2 [0.125 + \cos\sigma_d] (L/D)_d}{[39.88 - 11.78\cos(i)]1.125} \tag{14}$$

The total stagnation point heat load can be approximated for this type of trajectory within about 5% accuracy from

$$Q = 45{,}000 \frac{W/C_D A}{\dot{Q}_{\max}} \tag{15}$$

These equations can be used in the selection of the vehicle parameters L/D and $W/C_D A$, within the limits of this analysis. For example, a vehicle with a maximum heating rate of 80 Btu/ft^2·s, a dynamic pressure limit of 300 lb/ft^2, and a maximum of 3 G and a 2000 n.mi. crossrange requirement for a 90 deg inclined orbit yields an L/D of 1.84, a minimum bank angle of 43 deg, and a ballistic parameter of 225 lb/ft^2. This L/D and $W/C_D A$ define the "first cut" design point mentioned earlier.

Another example is the Shuttle orbiter, which has an 1100 n.mi. crossrange requirement resulting in an L/D of 1.342. Since the vehicle characteristics are known, this L/D corresponds to an angle of attack of about 33 deg and $W/C_D A$ equals 125 lb/ft^2. This ballistic parameter and L/D can be used with Eqs. (12) and (14) to yield a bank angle of 33.4 deg, a stagnation heating rate of 68 Btu/ft^2·s, and a heat load of 84,100 Btu/ft^2. This compares favorably with existing Shuttle data for entry at an angle of attack of 33 deg and a heating rate of 68 Btu/ft^2·s (scaled to a nose radius of 1 ft), but with a maximum of about 1.4 G.[24] This latter case yielded a heat load of about 90,000 Btu/ft^2. The 6.5% reduction in the heat load can be attributed to the steeper deceleration profile (3G) followed for the first case.

The effects of orbital inclination on crossrange were not studied closely. However, Eq. (3) can be used with Fig. 5 to approximate the effect. For a given heating limit and lift loading, the effect of the inclination on the bank angle can be found from Eq. (3). This change in bank angle will change the crossrange as shown in Fig. 5. For example, applying the first sample case to a 180 deg inclination results in a minimum bank angle of 10.2 deg to satisfy the heating constraint. For an L/D of 2.0 at 2000°F, going from a minimum bank angle of 43 to 10 deg translates to about a 10% reduction in crossrange capability. Thus at a 180 deg inclination with the same heating constraint, the crossrange capability is about 1800 n.mi.

Study Limitations

If the constant L/D assumption were lifted, more optimum trajectories might result. Flying a high drag profile during early entry, followed by pitchdown to a higher L/D after maximum heating may yield a lower heat load and still satisfy all other vehicle constraints. However, specific vehicle characteristics such as L/D vs Mach number and angle of attack cannot be found until a concept has been selected. After using a "first cut" design point to define a concept, a more optimum entry trajectory should be generated.

The impact that the load factor and dynamic pressure limits have on vehicle performance for a peak deceleration trajectory was not examined closely. However, in general increasing the G or q limits will decrease the total range, the stagnation heat load, and the entry flight time. [The range reduction can be estimated from Eqs. (6-8) by using any new limits on G or q.]

Transition to turbulent flow may occur, resulting in increased heat load and possibly an increase in the peak heating rate. To alleviate these problems a more gradual entry profile may have to be flown for segments of the trajectory. This would increase the stagnation heat load, but would tend to decrease the lower surface heat load by alleviating the higher turbulent heating.

The assumption that the local-to-stagnation heating rate ratio is less than or equal to 0.2 should be used only as an indicator of the local heating conditions on the vehicle. As a vehicle concept takes shape, specific flowfield characteristics can be used to find the actual local heating conditions.

Experience in the design of the Shuttle orbiter has demonstrated that a minimum heat load trajectory (peak deceleration) may not yield a minimum-weight vehicle because the coupling of airloads with thermal loads may result in a higher vehicle weight. For a metallic TPS reducing the total heat load tends to increase the peak heating rates and the total mass requirement. However, for any vehicle with some known maximum TPS surface temperature limit, this type of trajectory yields the shortest entry flight time and minimum stagnation heat load that the vehicle can safely attain.

Summary and Conclusions

Within the scope of this analysis, the peak deceleration entry profile is a viable alternative to glide-type trajectories when comparing crossrange capabilities and is more favorable when considering the total heat load that the vehicle's thermal protection system must be able to withstand. This is especially useful for an insulative TPS, since the TPS weight requirement tends to decrease with the heat load.

The methods presented here for selecting L/D and $W/C_D A$ to satisfy heating constraints while limiting the vehicle to 3 G

or 300 lb/ft^2 dynamic pressure could be used as an interactive preliminary design tool. Enough information was given to relate peak heating rate and orbit inclination with lift parameter [Eq. (3)], a crossrange requirement with L/D [Eq. (13)], L/D and peak heating rate with ballistic parameter [Eq. (14)], and peak heating rate and ballistic parameter with heat load [Eq. (15)]. Other relationships that would be useful as part of this preliminary design tool are given in Eqs. (6-8), for estimating the total range and Eq. (9) for equilibrium glide crossrange. All of this information except Eqs. (6-9) was verified from entry flight simulations using the POST computer program with the assumptions given earlier.

The information given here for selecting L/D and W/C_DA can be used to define a good "first cut" design point for an entry vehicle concept. Trades must then be made among vehicle volume requirements, areas, total weight, and the performance information presented before the final vehicle concept is drawn.

References

[1] Wurster, K.E., "Mass Reduction for Advanced Winged Entry Vehicles Through Integrated Thermostructural Trajectory Design," AIAA Paper 80-0363, Jan. 1980.

[2] Florence, D.E., "Selection of Hypersonic L/D to Minimize Thermal Protection System Weight and Meet Crossrange Requirements," AIAA Paper 79-1627, 1979.

[3] Bell, R.N., "A Closed Form Solution to Lifting Re-Entry," AFFDL-TR-6565, Jan. 1966.

[4] Slye, R.E., "An Analytical Method for Studying the Lateral Motion of Atmosphere Entry Vehicles," NASA TN D-325, Sept. 1960.

[5] Arthur, P.D. and Baxter, B.E., "Observations on Minor Circle Turns," *AIAA Journal,* Vol. 1, Oct. 1962, p. 2408.

[6] Chapman, D.R., "An Approximate Analytical Method for Studying Entry into Planetary Atmospheres," NASA TR R-11, 1959.

[7] Loh, W.H.T., *Re-Entry and Planetary Entry Physics and Technology,* Springer-Verlag, New York, 1968.

[8] Wagner, W.E., "Roll Modulation for Maximum Re-Entry Lateral Range," *Journal of Spacecraft,* Vol. 2, May 1965, p. 677.

[9] Wurster, K.E. and Eldred, C.H., "Technology and Operational Considerations for Low Heat-Rate Trajectories," AIAA Paper 79-0890, 1979.

[10] Dickmanns, E.D., "Maximum Range Three-Dimensional Lifting Planetary Entry," NASA TR R-387, 1972.

[11] Chern, J. and Vink, N., "Optimum Re-Entry Trajectories of a Lifting Vehicle," NASA CR 3236, 1980.

[12] Bursey, C., Johnson, D., and Nash, R., "Lifting Entry Vehicle Performance Analysis Methods," AIAA Paper 80-1665, Aug. 1980.

[13] Holloway, P.F. and Pritchard, E.B., "Atmospheric Maneuvers for Space Shuttles," Paper presented at AAS 16th Annual Meeting, June 1970.

[14] Knott, P.R. and Johnson, D.T., "Determination of Positions and Orientation Angles for a High L/D Glide Re-Entry to Hit a Predetermined Earth Target," AFFDL-TM-64-36, Oct. 1964.

[15] Galman, B.A., "Some Fundamental Considerations for Lifting Vehicles in Return From Satellite Orbit," *Proceedings of the Fourth AFBMD/STL Symposium,* Pergamon Press, New York, 1960.

[16] Eulberg, A.C., "A Translation of Manned Military Missions Into an Entry Vehicle Concept," AIAA Paper 65-488, 1965.

[17] Fennel, R.E., "Orbiter Entry Performance Data Book," Space Div., Rockwell International, SD 73-SH-0185, 1973.

[18] Rohsenow, W.M. and Hartnett, J.P., *Handbook of Heat Transfer,* McGraw-Hill Book Co., New York, 1973, pp. 1-3.

[19] Rakich, J.V. and Lanfranco, M.J., "Numerical Computation of Space Shuttle Laminar Heating and Surface Streamlines," *Journal of Spacecraft,* Vol. 14, May 1977, pp. 266-267.

[20] "Design and Analysis of the FDL-5 Reusable Spacecraft," AFFDL-TR-69-94, Dec. 1969.

[21] Thomas, A.C., Perlbachs, A., and Nagel, A.L., "Advanced Re-Entry Systems Heat Transfer Manual for Hypersonic Flight," AFFDL-TR-65-195, Oct. 1966.

[22] Brauer, G.L., Cornick, D.E., and Stevenson, R., "Capabilities and Applications of the Program to Optimize Simulated Trajectories (POST)," NASA CR-2770, Feb. 1977.

[23] Tamburro, M.B. and Knotts, E.F., "Entry Guidance Equations," North American Aviation, SID 66-1678-6, May 1967.

[24] "A Proposal to Accomplish Phase C, Space Shuttle Program," Space Div., Rockwell International, SD 72-SH-50-3, 1972.